Pharmacological Reports 71 (2019) 48–53

Contents lists available at ScienceDirect

Pharmacological Reports

journal homepage: www.elsevier.com/locate/pharep

Short communication

Insights into the structure and tubulin-targeted anticancer potential of N-(3-bromobenzyl) noscapine

Sanith Cheriyamundath[a], Tejashree Mahaddalkar[a], Praveen Kumar Reddy Nagireddy[b], Balasubramanian Sridhar[c], Srinivas Kantevari[b], Manu Lopus[a,*]

[a] School of Biological Sciences, UM-DAE Centre for Excellence in Basic Sciences, Mumbai, 400098, India
[b] Organic Chemistry Division-II (C P C Division), CSIR-Indian Institute of Chemical Technology, Hyderabad, Telangana 500007, India
[c] X-ray Crystallography, CSIR-Indian Institute of Chemical Technology, Hyderabad, Telangana 500007, India

ARTICLE INFO

Article history:
Received 16 March 2018
Received in revised form 6 August 2018
Accepted 5 September 2018
Available online 6 September 2018

Keywords:
Noscapine
N-BBN
X-ray crystallography
Tubulin
Microtubules
MDA-MB-231

ABSTRACT

Background: Noscapine is a non-narcotic, antitussive alkaloid isolated from plants of Papaveraceae family. This benzylisoquinoline alkaloid and its synthetic derivatives, called noscapinoids, are being evaluated for their anticancer potential.
Methods: The structure of a novel analogue, N-(3-bromobenzyl) noscapine (N-BBN) was elucidated by X-ray crystallography. Effect of N-BBN on cancer cell proliferation and cellular microtubules were studied by sulphorhodamine B assay and immunofluorescence, respectively. Binding interactions of the alkaloid with tubulin was studied using spectrofluorimetry.
Results: N-BBN, synthesized by introducing modification at site B ('N' in isoquinoline unit) and a bromo group at the 9th position of the parent compound noscapine, was found to be superior to many of the past-generation noscapinoids in inhibiting cancer cell viability and it showed a strong inhibition of the clonogenic potential of an aggressively metastatic breast tumour cell line, MDA-MB-231. The compound perturbed the tertiary structure of purified tubulin as indicated by an anilinonaphthalene sulfonic acid-binding assay. However, substantiating the common feature of noscapinoids, it did not alter microtubule polymer mass considerably. In cells, the drug-treatment showed a peculiar type of disruption of normal microtubule architecture.
Conclusion: N-BBN may be considered for further investigations as a potent antiproliferative agent.

Introduction

Tubulin, a heterodimeric, guanine nucleotide-binding protein, is the building block of the dynamic cellular filaments called microtubules. As the propagation of eukaryote cells depend on the proper assembly dynamics of tubulin, agents that perturb tubulin structure are considered potent anticancer drugs [1]. Currently-available tubulin-targeted anticancer drugs are associated with dose-limiting side effects such as toxicity to normal tissues [1], necessitating the development of novel, efficacious drug molecules.

Noscapine is a non-narcotic natural product alkaloid isolated originally from the opium poppy [2]. Noscapine and its congeners called noscapinoids, are potent anticancer compounds that show minimal side effects [3]. In order to enhance its efficacy, different structural alterations on the core noscapine skeleton have been considered (Fig. 1A) [4–6]. Many of these new generation noscapinoids have shown enhanced efficacy against a variety of cancer cell lines and tumours without being toxic to normal tissues [7].

Among the three major points that can be chemically manoeuvred (sites A, B and C; Fig. 1A), site A at 9th position on noscapine skeleton is most explored for introducing different groups. The first-generation noscapinoids thus synthesized included nitro, azido, amino, and halogenated (fluoro, chloro, bromo, and iodo) α-noscapine analogues [2]. These analogues showed considerably high anticancer activity [8,9]. Site B is the next most considered site for the chemical alteration. In early investigations, for example, Chandra group synthesized urea-type analogues through modification at this site (N–CH_3 group) and found a considerable anticancer activity for this analogue [7]. Thus, chemical alterations of the functional groups of noscapine have been shown to modulate its biological activity. In our ongoing efforts to design new noscapinoid derivatives with enhanced efficacy, we sought to introduce modification at site B ('N' in

* Corresponding author.
E-mail address: manu.lopus@cbs.ac.in (M. Lopus).

https://doi.org/10.1016/j.pharep.2018.09.002
1734-1140/

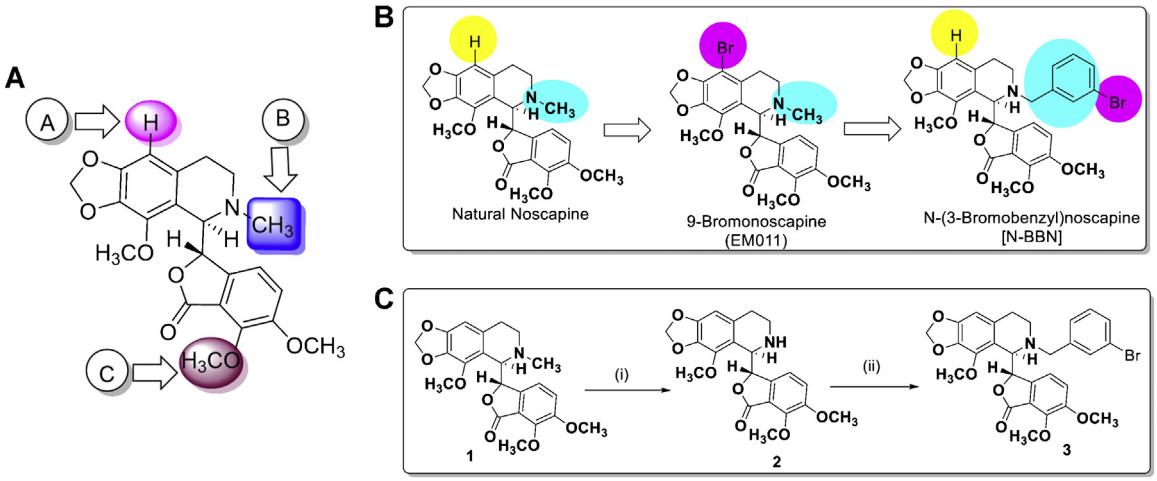

Fig. 1. A. Alteration points A, B and C on core skeleton of natural noscapine. B. The design strategy for N-BBN. C. Synthesis of nornoscapine **2** and N-BBN 3 from natural α-noscapine. Reaction conditions: (i) a: *m*CPBA, DCM; b: 2 N HCl; c: $FeSO_4.7H_2O$; (ii) 3-Bromo benzyl Bromide, KI, K_2CO_3, Acetone [10].

isoquinoline unit) of the parent compound. Further, considering the fact that introduction bromo group at the 9th position of noscapine enhanced its biological activity by several folds, we were curious to know the biological activity profile of a derivative in which "N" in isoquinoline unit, when functionalized with bromo-substituted benzyl unit [10]. Antitubulin agents have been found to be particularly effective against breast neoplasms [11]. For example, three major tubulin-targeted anticancer drugs in the market, Kadcyla [12], Ixempra [13], and Halaven [14] are used primarily for the treatment of breast neoplasms. We, therefore, chose the triple-negative breast cancer cell line, MDA-MB-231, for the cellular studies. We report structural elucidation of this compound (named, N-BBN) using single crystal X-ray diffraction, decipher the fine details of its interactions with tubulin, and evaluate its antiproliferative potential against MDA-MB-231 cells.

Materials and methods

Materials

Noscapine and sulforhodamine B were purchased from Sigma (St. Louis, MO, USA). All reagents were of analytical grade. Tubulin (microtubule-associated proteins-free tubulin) was purified from goat brain through multiple cycles of temperature- and GTP-dependent polymerization and depolymerization, as described earlier [15]. (*S*)-3-((*R*)-6-(3-bromobenzyl)-4-methoxy-5,6,7,8-tetrahydro[1,3]dioxolo[4,5-*g*]isoquinolin-5-yl)-6,7-dimethoxy isobenzofuran-1(3 H)-one, (N-BBN) was synthesized from natural noscapine and characterized in a manner similar as the one reported earlier [10].

X-ray crystallographic analysis of N-BBN

X-ray data of **N-BBN** was collected using a Bruker Smart Apex CCD diffractometer (Bruker, Billerica, MA, USA) with graphite monochromated MoKα radiation (λ = 0.71073 Å; ω-scan method) [16]. SAINT program was used for the integration and scaling of the intensity data. The **N-BBN** structure was solved using SHELXS97 through the direct method and was refined using the full-matrix least-squares technique (SHELXL97; [16]). We have included anisotropic displacement parameters for all atoms that are not hydrogen. All hydrogen atoms attached to carbon and nitrogen were positioned in difference fourier maps. They were then geometrically optimized and treated as riding on their parent atoms (C–H = 0.93-0.97 Å, N—H = 0.86 Å), with $U_{iso}(H) = 1.5U_{eq}(C)$ for methyl H or $1.2U_{eq}$(C, N). The methyl groups were allowed to rotate about the C—C bond without tipping.

Cell culture

The triple-negative breast cancer cell line, MDA-MB-231, was obtained from American Type Culture Collection (ATCC). The cells were cultured in Leibovitz's- L-15 medium (Himedia, India), in the presence of 10% fetal bovine serum (FBS; Gibco, Life Technologies, Carlsbad, CA, USA), and 1% penicillin and streptomycin (Life Technologies, Carlsbad, CA, USA) in a Forma Stericycle incubator (Thermo Scientific, Waltham, MA, USA) at 37 °C in the absence of CO_2.

Cell viability assay

Sulphorhodamine B (SRB) assay was performed for studying the effect of **N-BBN** on the cell viability. In brief, 2000 cells were seeded in each well of a 96-well cell culture plate and incubated overnight. Next day, the medium was replaced with fresh medium containing different concentrations of **N-BBN** (5 μM–50 μM) and the cells were incubated for 72 h. After the incubation, they were fixed with 10% (w/v) trichloroacetic acid (TCA) (4 °C; 1 h). After the fixation, the plates were washed thoroughly with distilled water, air dried, and stained with 0.4% SRB (w/v) in 1% acetic acid for 1 h. The unbound dye was then aspirated off and the wells were rinsed with 1% acetic acid and air dried. The protein-bound dye was then solubilized in 10 mM Tris base. Using a 96-well plate reader (Tecan, Switzerland), the absorbance of the dissolved dye in each well was measured at 564 nm. From the absorbance values, the percentage viability of the cells was calculated.

Clonogenic assay

In general, the spread of cancer to different parts of the body depends mostly on the ability of cancer cells to establish new colonies at sites that are proximal and distal to the site of an original tumour. Therefore, we next examined the potential of **N-BBN** in inhibiting the clonogenic propagation of this aggressively metastatic cancer cell line. For this assay, 800 cells were seeded on surface-treated 6-well cell culture plates and incubated overnight. The next day, the cells were exposed to increasing concentrations of **N-BBN** (5 μM–40 μM) for 8–10 days. The colonies formed at the end of this period were fixed with 3.7% formaldehyde and stained with 0.5% crystal violet for 2 h. After aspirating off

the dye, the wells rinsed thoroughly with distilled water. The colonies were photographed using a digital camera and were counted manually.

Immunofluorescence visualization of the microtubules and the DNA

For visualization of microtubules, the cells were seeded at a density of 2×10^4 cells/mL on surface-treated coverslips (Himedia, India) and incubated overnight. Next day, the cells were treated with **N-BBN** (0–28 μM) or with nocodazole (0.5 μM) for 24 h. The cells were then fixed using 3.7% formaldehyde at 25 °C for 20 min and permeabilized with chilled methanol (4 °C; 15 min). Nonspecific binding sites were blocked using 5% horse serum (1 h, 25 °C). The cells were then stained with mouse anti-α tubulin antibody (Sigma; 1:300 dilutions; 1 h, 25 °C) and then with an Alexa-568-conjugated goat anti-mouse antibody (Molecular Probes, Eugene, OR, USA; 1:1000 dilutions, 1 h, 25 °C). DNA was stained with Hoechst 33,342 (1 μg/mL; Molecular Probes, OR, USA). The coverslips were mounted on slides using Prolong Gold antifade reagent (Molecular Probes, OR, USA) and observed under Nikon 90i fluorescence microscope (Nikon, Minato, Japan).

Effect of N-BBN on tubulin structure

To examine the effect of **N-BBN** on the structural integrity of tubulin, an aniline naphthalene sulfonate (ANS) binding assay was performed [17]. Briefly, tubulin (2 μM) was incubated with **N-BBN** (0–80 μM) at 35 °C for 30 min in PEM buffer (50 mM PIPES, pH 6.8, 3 mM $MgSO_4$, 1 mM EGTA. Then ANS (50 μM) was added to this reaction mixture and incubated at 25 °C for 15 min in dark. Fluorescence measurements were taken after exciting the samples at 380 nm (emission wavelength range, 400–550 nm).

Effect of N-BBN on tubulin assembly in vitro

Tubulin (12 μM) was assembled in PEM buffer containing 1 mM, induced by 1 M sodium glutamate, at 35 °C for 45 min in a water-circulating bath, in the absence and presence of **N-BBN** (0–100 μM). The samples were then centrifuged, and the protein concentration in the pellets was measured using a Bradford assay with bovine serum albumin as the standard [15].

Results

Synthesis of N-BBN

As reported earlier [10], by reacting natural α-noscapine with *meta*-chloroperbenzoic acid (*m*CPBA) and by its subsequent acidification N-oxide HCl salt was generated. By treating the salt with Iron(II) sulfate heptahydrate ($FeSO_4.7H_2O$) (non-classical Polonovski reaction conditions), N-demethylated noscapine 2 (nornoscapine) was produced. Here, a partial change in reaction conditions has improved nornoscapine yield significantly. The nornoscapine was further functionalized with 3-bromobenzyl bromide in the presence of potassium carbonate to yield N-BBN 3 (98% yield) (Fig. 1). Nornoscapine 2 and **N-BBN** 3 were fully characterized by their IR, ^{1}H and ^{13}C NMR and mass spectral data as reported earlier [10].

Single crystal X-ray for N-BBN

Given the complexity of noscapine architecture, the structure of **N-BBN** was further characterized by its single crystal X-ray analysis (Fig. 2). The X-ray coordinates were deposited in the Cambridge crystallographic data centre and CCDC944744 obtained contains all supplementary crystallographic data for the structure of **N-BBN**. $C_{28}H_{26}BrNO_7$, $M = 568.41$, colorless block, $0.15 \times 0.13 \times 0.05$ mm^3, triclinic, space group $P1$ (No. 1), $a = 8.6602$ (11), $b = 12.3908(16)$, $c = 13.1081(16)$ Å, $\alpha = 72.095(2)$, $\beta = 73.337$ (2), $\gamma = 82.367(2)°$, $V = 1280.7(3)$ Å^3, $Z = 2$, $D_c = 1.474$ g/cm^3, $F_{000} = 584$, CCD Area Detector, MoKα radiation, $\lambda = 0.71073$ Å, $T = 294(2)$K, $2\theta_{max} = 50.0°$, 12,239 reflections collected, 8794 unique ($R_{int} = 0.0235$). Final *GooF* = 0.956, *R1* = 0.0499, *wR2* = 0.1266, *R* indices based on 6576 reflections with I I>2(I) (refinement on F^2), 673 parameters, 3 restraints, $\mu = 1.653$ mm^{-1}. Absolute structure parameter = 0.006(8).

N-BBN inhibited viability and clonogenic potential of cancer cells

After the synthesis and structure elucidation, we assayed its antiproliferative efficacy using an SRB assay. The data therefrom indicated that, 72 h treatment with **N-BBN** inhibits the viability of MDA-MB-231 cells in a concentration-dependent manner (Fig. 3A).

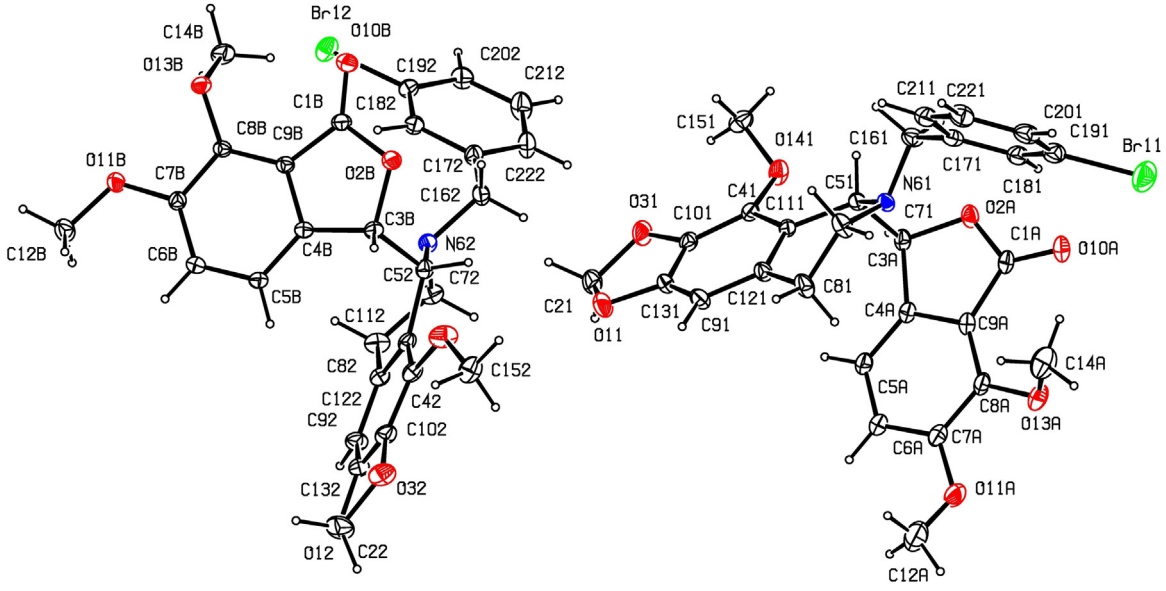

Fig. 2. ORTEP representations of **N-BBN** with thermal displacement ellipsoids drawn at the 30% probability level and H atoms are represented by circles of arbitrary radii.

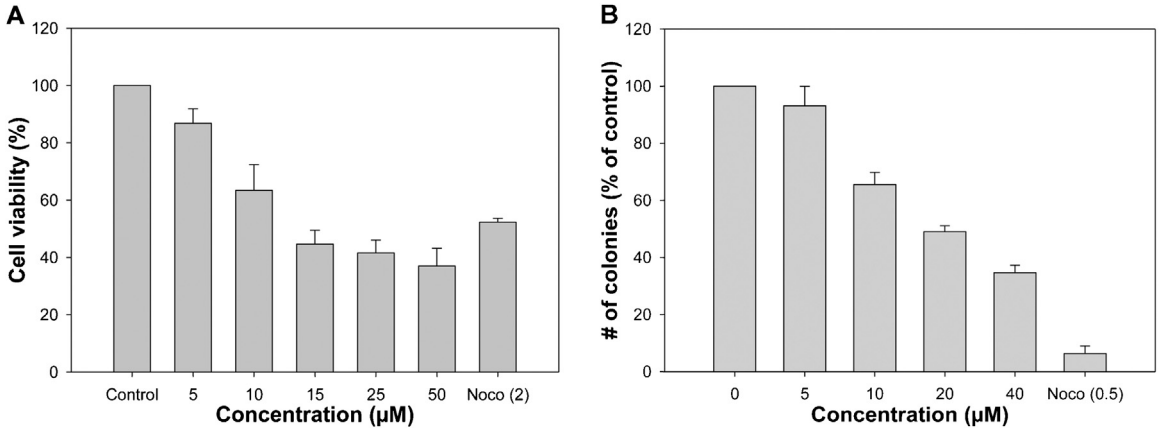

Fig. 3. A. Inhibition of MDA-MB-231 cell viability by **N-BBN**. Data, mean ± SD of three experiments. B. Inhibition of clonogenic propagation of MDA-MB-231 cells by **N-BBN**. Data, mean ± SD of three experiments. *Noco*, nocodazole.

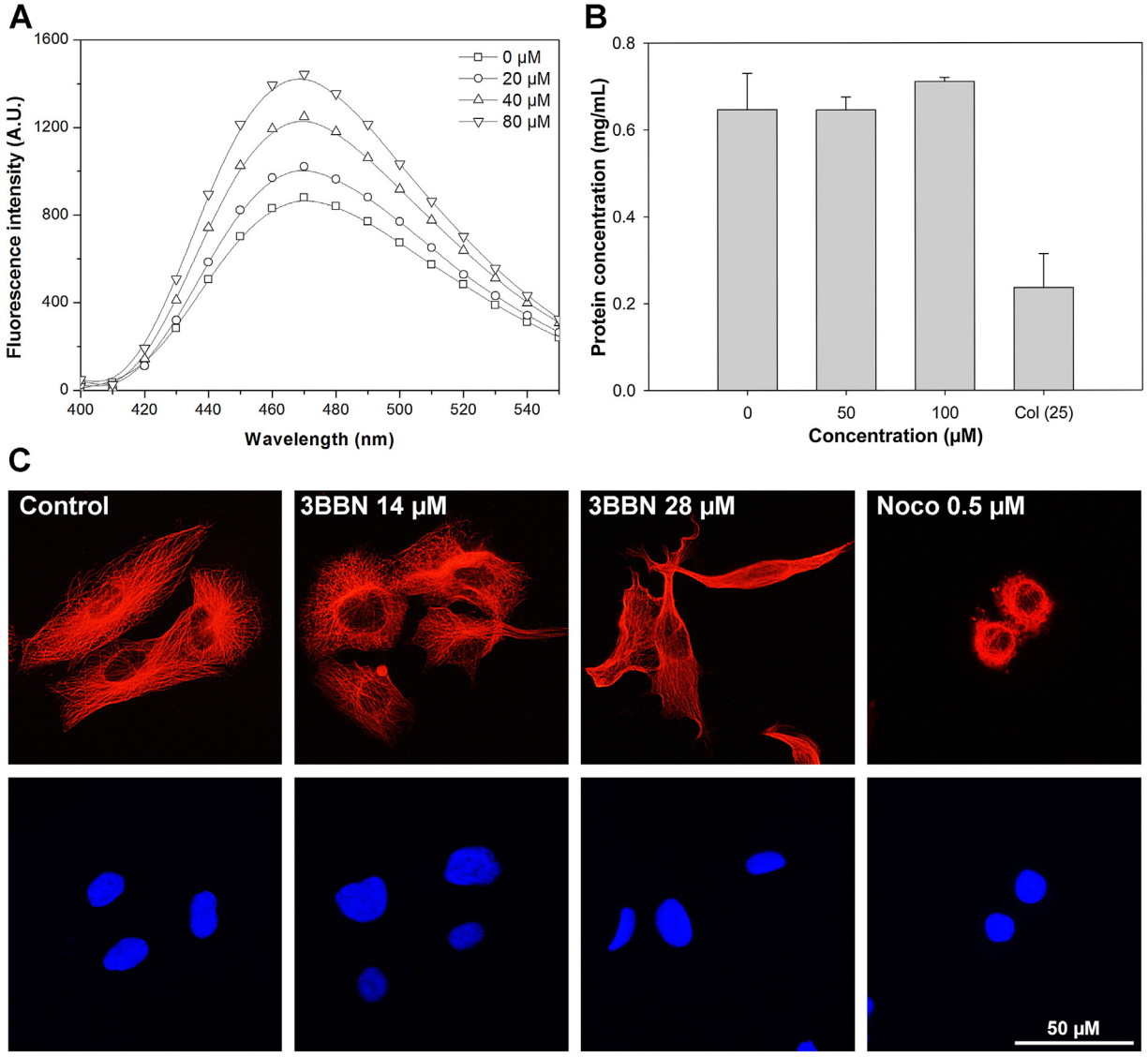

Fig. 4. A. Enhancement of tubulin-ANS fluorescence by **N-BBN** indicating the drug's direct binding to tubulin and the binding-induced structural perturbation of tubulin. The graph represents data from one of the three independent experiments. B. Effect of **N-BBN** on microtubule polymer mass. The noscapinoid did not alter the net polymer mass. Data, mean ± SD of three experiments. C. Effect of **N-BBN** on cellular microtubules. **N-BBN** damaged the structural integrity of the microtubules (red) without inducing apparent defects on DNA (blue) organization. *Noco*, nocodazole (For interpretation of the references to colour in this figure legend, the reader is referred to the web version of this article).

For example, 5 μM, 10 μM, and 25 μM **N-BBN** inhibited the cell viability by 13%, 37%, and 59%, respectively. The IC_{50} (half-maximal inhibitory concentration) was found to be 13 ± 1 μM. Since the noscapinoid showed a considerable antiproliferative potential, we examined its ability to inhibit the clonogenic potential of MDA-MB-231 cells. The drug inhibited the colony-forming ability of MDA-MB-231 in a concentration-dependent manner (Fig. 3B). Compared to the control, 5 μM, 10 μM, 20 μM, and 40 μM **N-BBN** inhibited the clonogenic capacity of triple negative breast cancer cell line by 7%, 35%, 51% and 65% respectively, further indicating its anticancer efficacy.

Disruption of tubulin structure by N-BBN

Investigating further into its mechanism of action, it was found that **N-BBN** increases the tubulin-ANS fluorescence in a concentration-dependent manner, indicating the drug's ability to expose hydrophobic patches on tubulin (Fig. 4A). For example, compared to the control, 20 μM, 40 μM and 80 μM of **N-BBN** increased the ANS-tubulin fluorescence by 16%, 42%, 64%, respectively, indicating that it perturbs the structural integrity of tubulin.

N-BBN did not inhibit microtubule polymer mass

Next, we examined if the perturbation of the structural integrity of tubulin induced by **N-BBN** affects its ability to assemble (Fig. 4B). A polymer mass assay indicated that the noscapinoid has a negligible effect on the net polymer mass, suggesting that, like other noscapinoids, **N-BBN** does not alter the microtubule polymer mass considerably.

Disruption of cellular microtubules

Immunofluorescence images of **N-BBN**-treated cellular microtubules showed a concentration-dependent disruption of the microtubule network (Fig. 4C). Compared to the control, the cells treated with 14 μM **N-BBN** (near the IC_{50}), showed apparent distortions of the microtubule network. At 28 μM (double the IC_{50}), the treated cells showed gross deformation of the cellular microtubule network, indicating that the noscapinoid damaged the structural integrity of the microtubule networks.

Discussion

We report the improved synthesis, X-ray crystallography-assisted structure elucidation, and biological evaluation of a rationally designed noscapine analog, (*S*)-3-((*R*)-6-(3-bromobenzyl)-4-methoxy-5,6,7,8-tetrahydro-[1,3]dioxolo[4,5-*g*]isoquinolin-5-yl)-6,7-dimethoxy isobenzofuran-1(3*H*)-one (**N-BBN**). The choice of benzyl group was to maintain the electronic environment around nitrogen in isoquinoline moiety on noscapine core intact (Fig. 1B). The bromo substituent was chosen because of the experimental evidence that 9-bromo noscapine has effective anticancer activity profile [9]. The preparation of noscapine derivative **N-BBN** (**3**) (Fig. 1C) involved peroxide-mediated N-demethylation of natural noscapine to give nornoscapine 2, and then derivatization with 3-bromobenzyl bromide in the presence of the base. The procedure presented here was optimized from the earlier protocol reported by our lab [10]. Due to the complexity of noscapine structure and the sensitivity of the C—C bond between two heterocyclic lobs, alkylation was carried out using weaker, carbonate-type bases. Specifically, potassium carbonate in the presence of potassium iodide in acetone was found to be the best choice here; alkylation proceeded well at 25 °C, to give the product in excellent yield (98%) (>96% HPLC purity). By spectral analyses [10] and X-ray crystallography (Fig. 2), we next elucidated the structure of this noscapinoid. Fig. 2 represents the ORTEP (Oak Ridge Thermal Ellipsoid Plot Program) diagram with two different orientations of **N-BBN** to correlate the stereochemistry around C—C bond between two heterocyclic lobs. The structure and stereochemistry of noscapinoid **N-BBN** were correlated with the stereochemistry of natural noscapine and unambiguously confirmed with the assigned structure for **N-BBN**.

After resolving the structure, we investigated the anticancer efficacy of this novel, rationally-designed noscapine derivative on one of the most aggressive human triple-negative breast cancer cell lines, MDA-MB-231. Compared to the IC_{50} of noscapine for MDA-MB-231 cell proliferation (36 μM; [18]), **N-BBN** showed three times less IC_{50}, (13 ± 1 μM) indicating its superior efficacy over the parent compound. The compound also inhibited the clonogenic propagation potential of the cells. Next, we investigated the details of its interaction with tubulin, the building block protein of microtubules, using spectrofluorimetry. An ANS binding assay indicated a concentration-dependent disruption of the tertiary structure of tubulin by the **N-BBN** (Fig. 4A). ANS binds hydrophobic patches on proteins and an enhancement in tubulin-ANS fluorescence is an indicator of a loss of structural integrity of the protein [19]. Despite perturbing the structural integrity of tubulin, the compound did not inhibit microtubule polymer mass (Fig. 4B). Thus, **N-BBN** shows retention of the effect of several noscapinoids on microtubule polymer mass. We then studied the intracellular manifestations of tubulin–**N-BBN** interactions. In cells, tubulin–**N-BBN** interactions were manifested as a disorganized microtubule network. The drug-treated microtubules showed "candle-flame-in-the-wind" morphology with a shrunken network without gross depolymerization of microtubules. The 'gentle yet effective' impact of **N-BBN** on cellular microtubules and cancer cell proliferation warrant further evaluation of this compound as an antiproliferative agent.

Conflict of interests

None to be declared

Acknowledgements

The authors thank UM-DAE Centre for Excellence in Basic Sciences (ML) and DBT-Indo-Australia biotechnology fund (BT/Indo-Aus/07/06/2013) (SK) for the financial support. The funding agencies did not demand or involve in study design, in the collection, analysis, and interpretation of data, in the writing of the report; or in the decision to submit the article for publication.

References

[1] Mahaddalkar T., Lopus M. From natural products to designer drugs: development and molecular mechanisms action of novel anti-microtubule breast cancer therapeutics. Curr Top Med Chem 2017;17:2559–68.
[2] Lopus M, Naik PK. Taking aim at a dynamic target: Noscapinoids as microtubule-targeted cancer therapeutics. Pharmacol Rep 2015;67:56–62.
[3] Karna P, Rida PC, Pannu V, Gupta KK, Dalton WB, Joshi H, et al. A novel microtubule-modulating noscapinoid triggers apoptosis by inducing spindle multipolarity via centrosome amplification and declustering. Cell Death Differ 2011;18:632–44.
[4] Naik PK, Lopus M, Aneja R, Vangapandu SN, Joshi HC. In silico inspired design and synthesis of a novel tubulin-binding anti-cancer drug: folate conjugated noscapine (Targetin). J Comput Aided Mol Des 2012;26:233–47.
[5] Mishra RC, Gundala SR, Karna P, Lopus M, Gupta KK, Nagaraju M, et al. Design, synthesis and biological evaluation of di-substituted noscapine analogs as potent and microtubule-targeted anticancer agents. Bioorg Med Chem Lett 2015;25:2133–40.
[6] Santoshi S, Manchukonda NK, Suri C, Sharma M, Sridhar B, Joseph S, et al. Rational design of biaryl pharmacophore inserted noscapine derivatives as potent tubulin binding anticancer agents. J Comput Aided Mol Des 2015;29:249–70.
[7] Tomar V, Kukreti S, Prakash S, Madan J, Chandra R. Noscapine and its analogs as chemotherapeutic agents: current updates. Curr Top Med Chem 2017;17:174–88.

[8] DeBono A, Capuano B, Scammells PJ. Progress toward the development of Noscapine and derivatives as anticancer agents. J Med Chem 2015;58:5699–727.
[9] Rida PC, LiVecche D, Ogden A, Zhou J, Aneja R. The Noscapine chronicle: A pharmaco-historic biography of the opiate alkaloid family and its clinical applications. Med Res Rev 2015;35:1072–96.
[10] Manchukonda NK, Naik PK, Santoshi S, Lopus M, Joseph S, Sridhar B, et al. Rational design, synthesis, and biological evaluation of third generation alpha-noscapine analogues as potent tubulin binding anti-cancer agents. PLoS One 2013;8:e77970.
[11] Fornier MN. Approved agents for metastatic breast cancer. Semin Oncol 2011;38:S3–10.
[12] Lopus M, Oroudjev E, Wilson L, Wilhelm S, Widdison W, Chari R, et al. Maytansine and cellular metabolites of antibody-maytansinoid conjugates strongly suppress microtubule dynamics by binding to microtubules. Mol Cancer Ther 2010;9:2689–99.
[13] Lopus M, Smiyun G, Miller H, Oroudjev E, Wilson L, Jordan MA. Mechanism of action of ixabepilone and its interactions with the betaIII-tubulin isotype. Cancer Chemother Pharmacol 2015;76:1013–24.
[14] Wilson L, Lopus M, Miller HP, Azarenko O, Riffle S, Smith JA, et al. Effects of eribulin on microtubule binding and dynamic instability are strengthened in the absence of the betaIII tubulin isotype. Biochemistry 2015;54:6482–9.
[15] Mahaddalkar T, Suri C, Naik PK, Lopus M. Biochemical characterization and molecular dynamic simulation of beta-sitosterol as a tubulin-binding anticancer agent. Eur J Pharmacol 2015;760:154–62.
[16] Sheldrick GM. A short history of SHELX. Acta Crystallogr A 2008;64:112–22.
[17] Mahaddalkar T, Mehta S, Cheriyamundath S, Muthurajan H, Lopus M. Tryptone-stabilized gold nanoparticles target tubulin and inhibit cell viability by inducing an unusual form of cell cycle arrest. Exp Cell Res 2017;360:163–70.
[18] Chougule MB, Patel AR, Jackson T, Singh M. Antitumor activity of Noscapine in combination with Doxorubicin in triple negative breast cancer. PLoS One 2011;6:e17733.
[19] Kundu B, Guptasarma P. Use of a hydrophobic dye to indirectly probe the structural organization and conformational plasticity of molecules in amorphous aggregates of carbonic anhydrase. Biochem Biophys Res Commun 2002;293:572–7.